International Journal of Geo-Information

MDPI

Article

Spatiotemporal Variation of NDVI in the Vegetation Growing Season in the Source Region of the Yellow River, China

Mingyue Wang [1,2], Jun'e Fu [2,3,*], Zhitao Wu [1] and Zhiguo Pang [2,3]

1 Institute of Loess Plateau, Shanxi University, Taiyuan 030006, China; sxwmyue@163.com (M.W.); wuzhitao@sxu.edu.cn (Z.W.)
2 China Institute of Water Resources and Hydropower Research, Beijing 100038, China; pangzg@iwhr.com
3 Research Center on Flood & Drought Disaster Reduction of the Ministry of Water Resources, Beijing 100038, China
* Correspondence: fuje@iwhr.com

Received: 27 February 2020; Accepted: 22 April 2020; Published: 24 April 2020

Abstract: Research on vegetation variation is an important aspect of global warming studies. The quantification of the relationship between vegetation change and climate change has become a central topic and challenge in current global change studies. The source region of the Yellow River (SRYR) is an appropriate area to study global change because of its unique natural conditions and vulnerable terrestrial ecosystem. Therefore, we chose the SRYR for a case study to determine the driving forces behind vegetation variation under global warming. Using the Normalized Difference Vegetation Index (NDVI) and climate data, we investigated the NDVI variation in the growing season in the region from 1998 to 2016 and its response to climate change based on trend analysis, the Mann–Kendall trend test and partial correlation analysis. Finally, an NDVI–climate mathematical model was built to predict the NDVI trends from 2020 to 2038. The results indicated the following: (1) over the past 19 years, the NDVI showed an increasing trend, with a growth rate of 0.00204/a. There was an upward trend in NDVI over 71.40% of the region. (2) Both the precipitation and temperature in the growing season showed upward trends over the last 19 years. NDVI was positively correlated with precipitation and temperature. The areas with significant relationships with precipitation covered 31.01% of the region, while those with significant relationships with temperature covered 56.40%. The sensitivity of the NDVI to temperature was higher than that to precipitation. Over half (56.58%) of the areas were found to exhibit negative impacts of human activities on the NDVI. (3) According to the simulation, the NDVI will increase slightly over the next 19 years, with a linear tendency of 0.00096/a. From the perspective of spatiotemporal changes, we combined the past and future variations in vegetation, which could adequately reflect the long-term vegetation trends. The results provide a theoretical basis and reference for the sustainable development of the natural environment and a response to vegetation change under the background of climate change in the study area.

Keywords: vegetation; partial correlation analysis; trend prediction; the source region of the Yellow River

1. Introduction

Global environmental change, which is marked by "global warming", has possible serious impacts on ecosystems and has attracted great attention from scientists around the world [1,2]. Vegetation cover is an important component of the environment, and is also the best indicator of the regional ecological environment [3]. The variation in vegetation cover is the direct result of environmental change [4]. As the main component of terrestrial ecosystems, vegetation is a sensitive indicator of

climate change. Therefore, in the context of global climate change, it is of great significance to identify the spatiotemporal characteristics of vegetation cover to regulate ecological processes and ensure ecological security.

The Normalized Difference Vegetation Index (NDVI) can be used to measure the improvement and degradation of vegetation cover. NDVI is a good satellite-based indicator of vegetation at the landscape scale [5,6]. The NDVI time series intuitively reflects the vegetation growth and coverage status. The NDVI is widely used in global and regional vegetation change research. Kawabata et al. found that vegetation activities increased remarkably in the northern middle-high latitudes [7]. Relevant research has shown that the vegetation in China has exhibited the same trend. Liu et al. analysed the vegetation changes in China from 1982 to 2012. The results showed that the NDVI exhibited a slowly increasing trend with obvious regional characteristics. The increasing trend slowed after 1997 [8]. Piao and Fang used global inventory modeling and mapping studies (GIMMS) NDVI data to analyse the vegetation cover in China from 1982 to 1999, and showed that 86.2% of China's area exhibited an increasing trend in vegetation. The changes in NDVI were significantly affected by climate fluctuations and had obvious regional differences [9]. Xu et al. analysed the vegetation coverage from 2000 to 2015 and showed that the area with increased vegetation coverage accounted for 83.34% of the area in China [10]. Other scholars have performed extensive research on vegetation cover changes in the Huang-Huai-Hai River basin [11], in the Yangtze River basin [12], on the Qinghai–Tibet Plateau [13], and in the southwestern karst region [14]. The above research showed that the vegetation increased in regional areas or throughout whole countries. The Qinghai–Tibet Plateau was shown to be more sensitive to the effects of climate warming than other regions.

The source region of the Yellow River (SRYR) is located on the sensitive margin of the northeastern Qinghai–Tibet Plateau [15]. Most of this region are located between 4200 and 5000 m above sea level, and the percentage of the area above 5000 m is less than 1% [16]. The main vegetation is grassland, including alpine grassland and alpine meadow, which cover 74.55% of this region. The region is an important part of the terrestrial ecosystem of the Qinghai–Tibet Plateau. The SRYR is also a water conservation area and a key protected area in the Yellow River basin [17]. With the rise of ecological protection in the Yellow River basin as a major national strategy [18], it is of great significance to dynamically monitor the spatiotemporal evolution of surface vegetation cover. Over the past decades, the region has experienced severe climate change. Many studies have indicated that the temperature and precipitation in the study area have increased [19,20], and the vegetation coverage has exhibited a tendency of restoration because the climate has become gradually warm and wet [21]. Some researchers have studied the relationships between vegetation coverage and environmental variation [22]. Guo et al. found that vegetation cover changes in the SRYR showed very impressive correlations with climatic factors [23]. Liang et al. reported that local hydrological conditions directly influenced vegetation variations, and overgrazing can be a leading cause of localized vegetation degradation [24]. Most of the studies on the vegetation coverage in the study area have focused on current interannual changes, while few studies have focused on different regions and the future.

Land-use types represent the ongoing challenges of environmental variation and the impacts of human activities [25]. Therefore, based on the NDVI data and climate data from 1998 to 2016, this study analysed the spatiotemporal changes in the NDVI and the response mechanisms of different land-use types in the growing season and predicted them for the next 20 years. This study provides a scientific basis for the development of countermeasures to protect vegetation in the SRYR under the background of global warming.

2. Data and Methods

2.1. Study Area

The SRYR (32°09–36°34 N, 95°54–103°24 E) is located on the northeastern Qinghai–Tibet Plateau and covers an area of 131,400 km^2, accounting for 16.2% of the Yellow River basin area. The study

areas in this paper are shown in Figure 1. The administrative area mainly includes 17 counties in the three provinces of Qinghai, Gansu and Sichuan. The elevation in the SRYR decreases from west to east with a maximum altitude of 6253 m and a minimum of 2410 m. The lowest elevation of the study area exists in Longyangxia Reservoir, and the highest elevation is in the Anyemaqen Mountains. The region has a continental plateau climate, which is obviously affected by the southwest monsoon. The temperature and precipitation decrease from the southeast to the northwest. The annual average rainfall is approximately 530 mm yr^{-1} [26]. From the southeast to the northwest, the annual average daily temperature varies between 2 °C and −4 °C [27]. There are many glaciers and extensive permafrost as well as a large number of lakes and rivers, which feed a large number of marsh wetlands; these areas provide more than 40% of the runoff in the Yellow River basin [28]. The SRYR is an important water conservation area and is also known as a "plateau water tower".

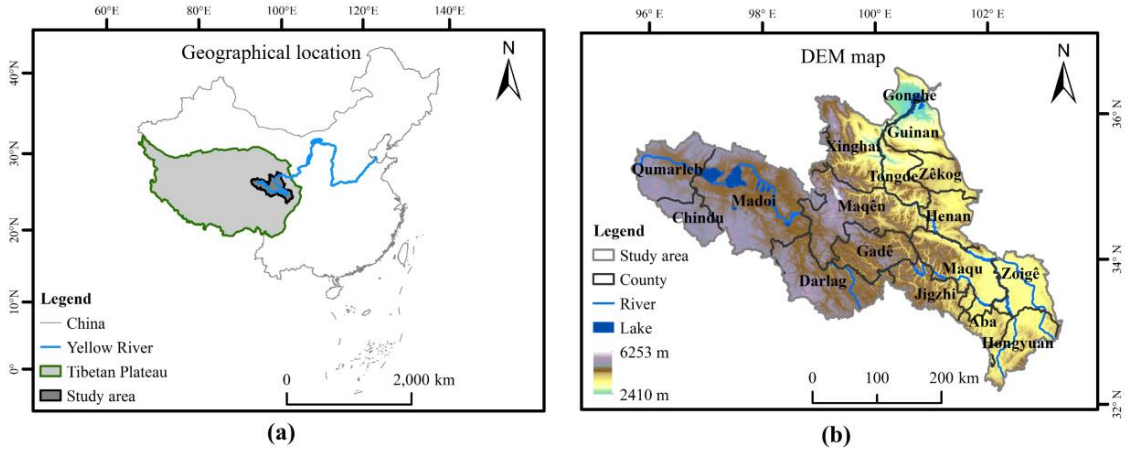

Figure 1. The source region of the Yellow River (SRYR): (**a**) geolocation location; (**b**) digital elevation model (DEM) map.

2.2. Data

The NDVI data used in this paper were provided by the Resources and Environment Science Data Center of the Chinese Academy of Sciences (http://www.resdc.cn). The data were based on NDVI time series data obtained from satellite remote-sensing images by SPOT/VEGETATION and moderate-resolution imaging spectroradiometer (MODIS). The data can reflect the distribution and change of vegetation cover in various regions of China on the spatiotemporal scales effectively, which is of great reference significance to the monitoring of vegetation variation, the rational utilization of vegetation resources and other researches on ecological environment [29]. The data were processed with atmospheric, radiation, and geometric corrections. The data were synthesized by using maximum value composites (MVC) with a spatial resolution of 1 km and a temporal resolution of one month. After verification, the accuracy was found to meet the requirements. The data have been used in research on monitoring vegetation dynamic changes. The average monthly NDVI values from May to September were used to obtain the annual NDVI values during the growing season from 1998 to 2016. The daily meteorological grid data were provided by the National Climate Center [30], including the CN05.1 data from 1998–2016 and the regional climate model version 4 (RegCM4) data from 2020–2038, which had spatial resolutions of 0.25° and 0.0625°, respectively. The climate elements included precipitation (Pre) and temperature (Tm). The daily values of the two climate elements were statistically estimated from May to September, and these data were resampled to a spatial resolution of 1 km to be consistent with the spatial resolution of the NDVI dataset. The data have been heavily cited in scientific papers [31]. The land-use types in 2015 were obtained from the Resources and Environment Science Data Center of the Chinese Academy of Sciences (http://www.resdc.cn), with a spatial resolution of 100 m. The land-use types were integrated into six categories: cropland, woodland, grassland, water bodies, built-up land and unused land.

2.3. Methods

The linear trend method [32] was used to analyse the NDVI trends. A positive slope indicated that the vegetation tended to improve with increasing NDVI. A negative slope indicated that the vegetation tended to deteriorate with decreasing NDVI. The statistic e_{slope} was calculated as in Equation (1) as follows:

$$e_{slope} = \frac{n \times \sum_{i=1}^{n} i \times NDVI_i - \sum_{i=1}^{n} i \times \sum_{i=1}^{n} NDVI_i}{n \times \sum_{i=1}^{n} i^2 - \left(\sum_{i=1}^{n} i\right)^2} \quad (1)$$

where e_{slope} represents the slope of the NDVI trend, i represents the year serial number, and n represents the time series length.

The Mann–Kendall abrupt test [33] was used to determine the year of the NDVI change. The statistics were defined under the assumption that the time series were random and independent. The UF_k statistic was calculated with the following equations:

$$UF_k = \frac{d_k - E(d_k)}{\sqrt{\mathrm{Var}(d_k)}} \quad (2)$$

where

$$d_k = \sum_{i=1}^{k} m_i, \ (2 \le k \le n) \quad (3)$$

$$m_i = \begin{cases} 1, \ NDVI_i > NDVI_j \\ 0, \ else \end{cases}, \ (1 \le j \le i) \quad (4)$$

$$E(d_k) = \frac{k(k-1)}{4} \quad (5)$$

$$\mathrm{Var}(d_k) = \frac{k(k-1)(2k+5)}{72} \quad (6)$$

where UF_1 is equal to 0. The d_k statistic is reduced to that given in Equations (3) and (4), which indicates that the value at time i was greater than the value at time j. Equation (5) calculates the mean of the UF_k statistic, and Equation (6) calculates the variance. Then, the order of column d_k is calculate as the reverse time series. The UB_k value was calculated according to the above equation. Given the significance level $\alpha = 0.05$, the critical value of the UB_k statistic was |1.96|. A sequence was constructed for 19 samples and the UF_k and UB_k curves and significant horizontal lines were drawn. If UF_k was greater than 0, it meant that the sequence showed an increasing trend, and a value of less than 0 indicated a decline. When the threshold exceeded |1.96|, it indicated that the trend was significant. If the UF_k and UB_k curves had intersection points within the confidence interval, the time corresponding to the intersection point was the possible change point.

In addition, this study used partial correlation analysis [20] to analyse the relationship between the climatic factors and the NDVI. The partial correlation coefficient is an index that measures the degree of linear correlation between the two variables by controlling the effects of multiple other variables. Moreover, this study used the residual analysis method [34,35] to analyse the impacts of human activities on the NDVI. Based on the NDVI, precipitation and temperature values from 1998 to 2016, the residual method was used to simulate the relationship between the NDVI and the climate elements for each pixel. The changes in the residuals in the NDVI predictions and observations reflected the contributions of human impacts to the actual changes in NDVI. Positive residuals indicated that the human impacts on vegetation were positive, and negative residuals indicated that the human impacts on vegetation were negative.

3. Results and Analysis

3.1. Spatiotemporal Variation in Normalized Difference Vegetation Index (NDVI)

Table 1 shows the basic situation of the main counties, which shows that water bodies and built-up land accounted for a small proportion, so vegetation variations in these land-use types will not be subsequently analysed. Among the different land-use types, the proportion of grassland in the region was the highest. Among the different counties, NDVI in Zoigê had the highest values.

Table 1. Normalized Difference Vegetation Index (NDVI) value and proportion of land-use types in different counties.

Countie	Mean NDVI Value	Land-Use Types/%					
		Crop-Land	Wood-Land	Grass-Land	Water Body	Built-Up Land	Unused Land
The source region of the Yellow River (SRYR)	0.486	0.94	6.77	74.45	2.27	0.13	15.44
Zoigê	0.674	0.03	0.75	70.44	1.07	0.27	27.44
Hongyuan	0.674	0.03	7.26	79.62	0.03	0.23	12.83
Aba	0.666	/	8.37	85.57	0.09	/	5.98
Henan	0.655	/	15.75	78.45	0.80	0.12	4.87
Maqu	0.640	/	8.10	73.75	1.72	0.09	16.34
Jigzhi	0.602	/	10.18	86.04	0.71	0.03	3.03
Zêkog	0.593	1.49	2.90	78.88	0.44	0.05	16.24
Gadê	0.558	/	12.72	82.55	0.62	0.03	4.08
Tongde	0.540	7.91	22.89	58.34	1.08	0.17	9.61
Maqên	0.485	0.02	16.29	68.29	1.88	0.12	13.40
Darlag	0.476	/	2.23	88.94	0.95	0.01	7.88
Xinghai	0.424	0.50	10.98	67.47	0.87	0.08	20.11
Guinan	0.410	11.14	2.43	65.73	3.00	0.21	17.49
Chindu	0.396	/	/	84.65	1.44	/	13.91
Madoi	0.324	/	0.20	74.21	7.22	0.01	18.36
Qumarleb	0.290	/	/	62.51	1.50	0.01	35.98
Gonghe	0.257	3.70	1.20	63.47	7.57	2.50	21.56

The spatial distribution of the NDVI in the growing season in the SRYR from 1998 to 2016 exhibited obvious regional differences. The spatial variability analysis showed an increasing gradient of NDVI from northwest to southeast in Figure 2a. The maximum NDVI value was 0.76, which was located in the Zoigê wetland. By referring to related studies [36], the NDVI values were classified into 5 levels. The NDVI distribution was analysed in combination with the land-use types (Figure 2c). The multiyear average NDVI in the growing season was 0.486, of which the area where NDVI was <0.1 covered 1.17% of the total area, mainly including water bodies represented by Eling Lake, Zaling Lake, and Longyangxia Reservoir and permanent glacial snow on the Anyemaqen Mountains. The area with NDVI values between 0.1 and 0.3 covered 15.12% of the area, mainly including unused land that was dominated by sand; the Gobi Desert; the marshlands in northern Qumarlêb, northern Madoi, and western Xinghai around Longyangxia Reservoir; and the sandy area in Huangshatou. The area where the NDVI was between 0.3 and 0.6 covered 50.77% of the area and was mainly distributed in Qumarleb, Madoi, Chindu, Maqên, Xinghai and Guinan, with medium- and low-coverage grassland. In addition, this area also included cultivated land in parts of Guinan. The NDVI values between 0.6 and 0.7 covered 27.90% of the total area. These areas were mainly located in the central counties of the region, which are dominated by medium- and low-coverage grasslands. The areas where NDVI was >0.7 covered 5.04% of the total area, mainly including Aba, Maqu, Zoigê, and Hongyuan, which have high-coverage grasslands and some medium-coverage grasslands.

The spatial distribution of the mean NDVI values can represent the overall trend of the vegetation, but there were opposite changes in different regions, and they can offset each other. Therefore, based on the unitary regression model, the trend of NDVI over the 19 years was analysed at the pixel scale. According to Figure 2b, the NDVI in the SRYR increased in most areas and decreased in some local areas.

According to the statistics, from 1998 to 2016, the area where the NDVI increased covered 71.40% of the total area. Among the areas with NDVI increases, the rapidly increasing area covered 33.12% of the total area and was mainly distributed in the southeast. The NDVI values did not change significantly in 19.41% of the areas. These areas were mainly distributed in Madoi, Gadê and Huangshatou in Guinan. As a typical aeolian sand control area, the trend of NDVI remained basically unchanged, which reflected the long-term and arduous nature of sandy land management. The reduced NDVI area covered 9.19% and was mainly distributed in Qumarleb (grasslands with medium and low coverage, unused land with bare rock), Maqên, and an urban area of Gonghe. The above studies indicated that while the state of vegetation in the SRYR had improved, some areas experienced vegetation degradation.

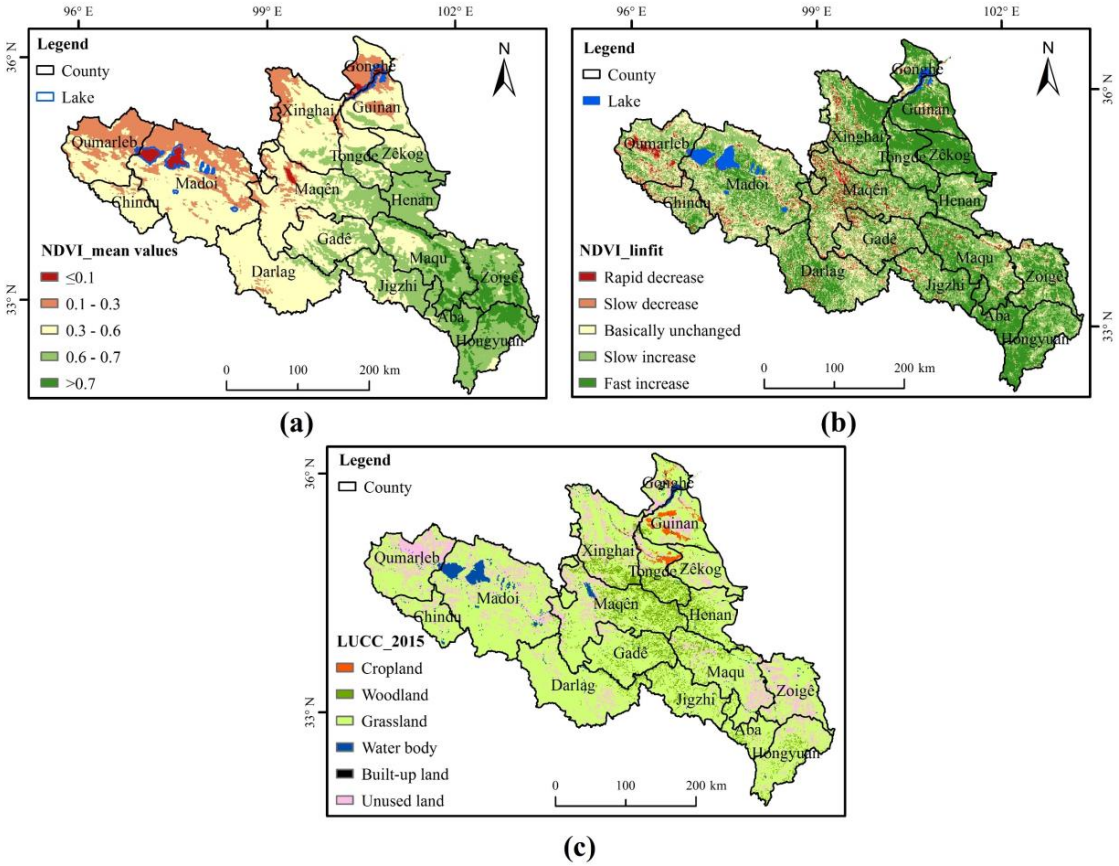

Figure 2. Spatial distribution in the SRYR from 1998 to 2016: (**a**) mean NDVI value; (**b**) NDVI change trend; (**c**) land-use types in 2015. In Figure 2b, rapid decrease represents a slope <–0.003; slow decrease represents –0.003 < slope < –0.001; basically unchanged represents –0.001 < slope < 0.001; slow increase represents 0.001 < slope < 0.003; rapid increase represents a slope <0.003.

As we can see in Figure 3, the NDVI in the SRYR increased slowly over the past 19 years, with a slope of 0.00204/a. Before 2005, the NDVI was lower than the multiyear average values, and then it fluctuated around the average, indicating that the vegetation coverage had improved since 2005. The State Council approved and launched the "master plan for ecological protection and construction of the Three-River-Source Nature Reserve in Qinghai" in 2005 and implemented a series of engineering measures. The results of this article showed that the implementation of these projects had a certain effect on vegetation restoration and protection. From the different land-use types, the trend of the grassland NDVI was the most consistent with that of the whole region. The NDVI values for different land-use types in the region showed an upward trend. The increasing trend of cropland NDVI was the most obvious, with a linear tendency of 0.00559/a, an average NDVI value of 0.46, and a change point that occurred in approximately 2004. Both the woodland NDVI and grassland NDVI showed

slow trends, with linear tendencies of 0.00248/a and 0.00214/a, respectively. The average woodland NDVI value was 0.60, and the change point was between 2009 and 2011. The average grassland NDVI value was 0.50, and the change point was approximately 2006. The unused land NDVI showed slight increasing trends, with linear tendencies of 0.00147/a, an average NDVI value of 0.40, and the abrupt point occurred in approximately 2003. In the study area, the unused land in the west mainly included sandy land and the Gobi with low NDVI values; the eastern part, namely, the Zoigê wetland, was dominated by marshland with high NDVI values. In summary, the distribution of the NDVI values in the different land-use types was woodland > grassland > cropland >> unused land. In terms of trends, the grassland NDVI contributed significantly to the annual NDVI in the study area.

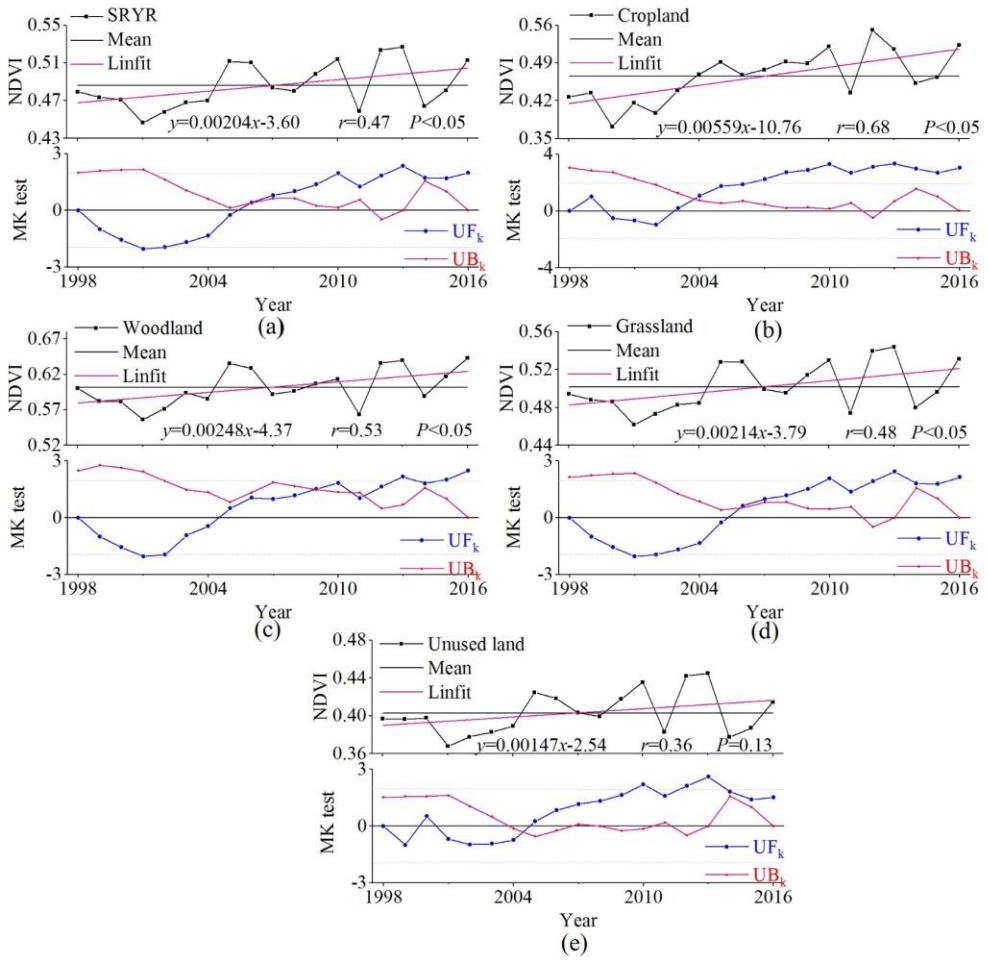

Figure 3. Temporal change of NDVI in different land-use types: (**a**) the SRYR; (**b**) cropland; (**c**) woodland; (**d**) grassland; (**e**) unused land.

The increasing trends in NDVI were obvious in many regions in China; however, the NDVI changes in the SRYR were relatively small, even though many protective measures were adopted by the government in the region at the same time, and increasing trends of climate change were faster than the average in China. Therefore, we discussed the main factors affecting NDVI in the subsequent analysis.

3.2. Impact of Meteorological Elements on the NDVI

Many studies have shown a clear response of NDVI to climate change. The impact of climate change on vegetation is mainly reflected in the hydrothermal conditions. Evapotranspiration data for long-term continuous observations are difficult to obtain. Therefore, climate change can be attributed as a cause of changes in precipitation and temperature. Temperature and precipitation are the most direct and important factors for plant growth [37,38]. Figure 4 shows that the precipitation in the growing

season showed an upward trend, with a linear trend of 7.17/a and an average value of 449.52 mm. The average temperature linearly increased at 0.04/a, with an average value of 6.42 °C. The precipitation and temperature were mainly below average before 2005. The precipitation had the lowest value in 2001. After 2005, the climate elements fluctuated around the mean value. The consistency between NDVI and temperature was better than the consistency between NDVI and precipitation.

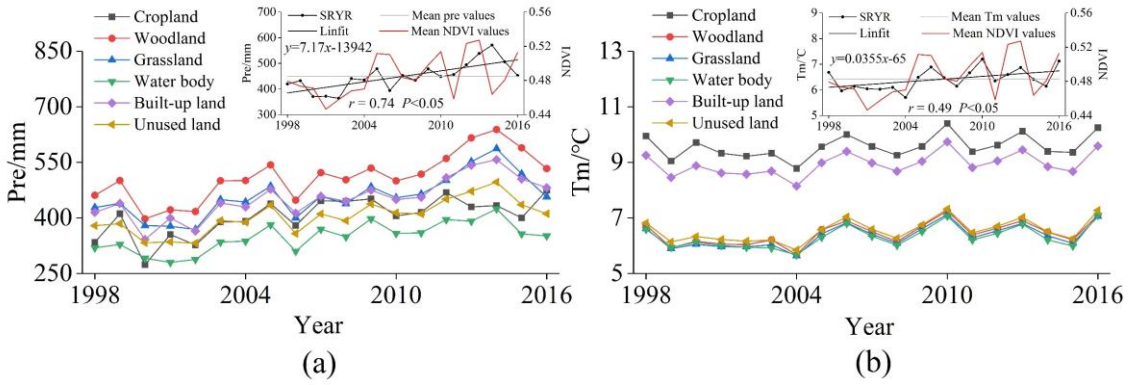

Figure 4. Temporal change in the climate elements from 1998 to 2016: (**a**) precipitation; (**b**) temperature.

Correlation coefficients between climate elements and NDVI in different land-use types are shown in Table 2. The partial correlation coefficient between the NDVI and precipitation was 0.221 (P = 0.289), and the coefficient between the NDVI and temperature was 0.467 (P = 0.131). Among the NDVI values for the different land-use types, precipitation exhibited the best correlation with cropland, and passed the 5% significance level test. Cropland mainly located in the central of Guinan and north of Tongde. The driving force of precipitation on cropland was stronger than temperature. Temperature had the best correlation with grassland, followed by woodland.

Table 2. Partial correlation coefficient.

Climate Elements	SRYR	Cropland	Woodland	Grassland	Unused Land
Pre	0.221	0.669 *	0.276	0.216	0.230
Tm	0.467	0.363	0.471	0.490	0.411

* indicates significance at the 5% level.

Table 3 shows the partial correlation between climate elements and NDVI in different counties. The correlation coefficient between precipitation and NDVI was positive in all counties. Among the different counties, at the significance level of 0.05, Guinan exhibited the highest significant correlation proportion that covered 71.08% of the total area, followed by Zêkog and Gonghe. The significant correlation proportion in these counties were all above 50%. The counties where the significant correlation proportion were between 25% and 50% were mainly distributed in Xinghai, Tongde, Madoi, Zoigê, Henan and Qumarleb. The counties where the significant correlation proportion were <25% mainly included Maqên, Hongyuan, Darlag, Maqu, Aba, Jigzhi, Gadê and Chindu.

Table 3. Climate elements and correlation coefficients in different counties.

Counties	Pre			Tm		
	Mean Value/mm	Correlation Coefficients	Significant Correlation Proportion/%	Mean Value/°C	Correlation Coefficients	Significant Correlation Proportion/%
SRYR	449.52	0.221	31.01	6.42	0.467	56.40
Zoigê	547.11	0.285	30.79	8.75	0.499	64.41
Hongyuan	623.22	0.257	24.30	7.96	0.556	75.39
Aba	609.28	0.206	19.24	8.27	0.588 *	83.15
Henan	512.34	0.332	28.92	7.19	0.524	72.32
Maqu	567.74	0.181	19.97	7.49	0.510	66.48
Jigzhi	633.57	0.066	17.13	6.00	0.541	74.71
Zêkog	459.47	0.519	62.79	7.50	0.550 *	81.04
Gadê	522.78	0.060	16.72	5.20	0.459	52.45
Tongde	447.81	0.443	45.50	7.95	0.442	47.50
Maqên	450.46	0.137	24.35	5.07	0.417	44.27
Darlag	494.39	0.084	24.02	5.14	0.535	70.44
Xinghai	376.10	0.372	46.62	6.76	0.292	16.94
Guinan	392.23	0.553	71.08	10.09	0.366	34.68
Chindu	350.83	0.036	11.72	4.29	0.560	72.07
Madoi	319.84	0.144	31.09	5.05	0.474	58.37
Qumarleb	267.72	0.228	27.97	4.87	0.456	53.48
Gonghe	379.30	0.439	54.92	11.00	0.252	10.80

* Indicates significance at the 5% level.

The counties where the significant correlation proportion between NDVI and temperature were above 75% mainly included Aba, Zêkog and Hongyuan. Aba exhibited the highest significant correlation proportion that covered 83.15% of the total area. Both Aba and Zêkog correlation coefficients passed the 5% significance level test. That is, the driving force of temperature on vegetation was stronger than precipitation in these areas. The counties where the significant correlation proportion were between 50% and 75% were mainly distributed in Jigzhi, Henan, Chindu, Darlag, Maqu, Zoigê, Madoi, Qumarleb and Gadê. The counties where the significant correlation proportion were between 25% and 50% were mainly included Tongde, Maqên and Guinan. The counties where the significant correlation proportion were <25% mainly included Xinghai and Gonghe. The contents of correlation coefficients are shown in Figure 5.

Figure 5 shows the relationship between NDVI, climatic elements and partial correlation coefficient in different counties. Precipitation and temperature were positively correlated with NDVI. That is, in different counties, the NDVI increased gradually with increasing precipitation and temperature. The higher the NDVI is, the weaker the correlation between precipitation and NDVI. The higher the NDVI is, the stronger the correlation between temperature and NDVI. Figure 5c,d show the partial correlation coefficient between climatic elements and NDVI. As shown in the figure, precipitation, temperature and the correlation coefficient were negatively correlated; that is, with the increase in precipitation and temperature, the correlation between NDVI and climatic factors weakened. In general, the lower the precipitation and temperature of the county were, the stronger the correlation between climate factors and NDVI. Generally, the effects on vegetation were more obvious under unfavourable climate conditions than under suitable ones.

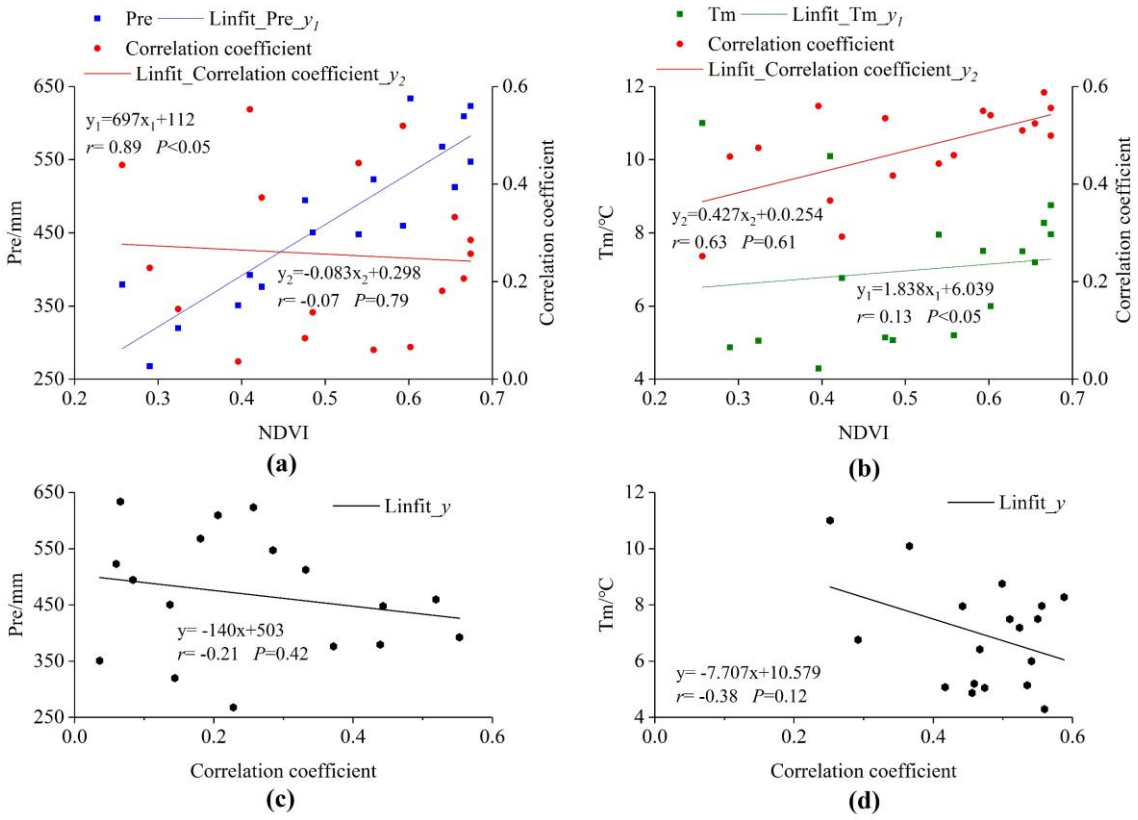

Figure 5. Correlation analysis in different counties for: (**a**) NDVI, precipitation, and correlation coefficient; (**b**) NDVI, temperature, and correlation coefficient; (**c**) precipitation and correlation coefficient; (**d**) temperature and correlation coefficient.

The spatial distribution of the partial correlation coefficient between the NDVI and climate elements in the growing seasons is shown in Figure 6. At the pixel scale, the partial correlation coefficient between the NDVI and precipitation showed a significant positive correlation with precipitation that covered 27.08% of the total area in Figure 6a. This correlation was mainly distributed in Guinan, which mainly includes grassland and sandy land, most of this region is located between 2559 and 4759 m above sea level, and the annual average precipitation is below 400 mm; significant positive correlations were also observed in Zêkog, Gonghe, Tongde, Xinghai, and northwestern Madoi. A total of 68.99% of the area was not significantly related. The areas with significant negative correlations covered 3.93% of the total area, and points were distributed in Darlag and Madoi. This region is located between 3787 and 5236 m above sea level, and the annual average temperature is below 5.5°C. There was an increase in precipitation and widespread melting of glaciers and snows, which fed glacial lakes and wetlands, reducing the vegetation coverage in glacial snow regions to a certain extent.

The area where there was a significantly positive correlation between NDVI and temperature covered 56.34% of the total area in Figure 6b, and was mainly distributed in Zêkog, the southern Madoi, Chindu, Darlag, and the southeastern SRYR. The area that was not significantly related covered 43.60%, and was mainly distributed in Gonghe, Xinghai, northern Guinan, Maqên and Gadê.

Overall, the NDVI exhibited a positive correlation with precipitation and temperature in the SRYR, and the correlation with temperature was higher than that with total precipitation. This result showed that the sensitivity of the NDVI to temperature was higher than that of precipitation, which showed that temperature had a greater impact on vegetation.

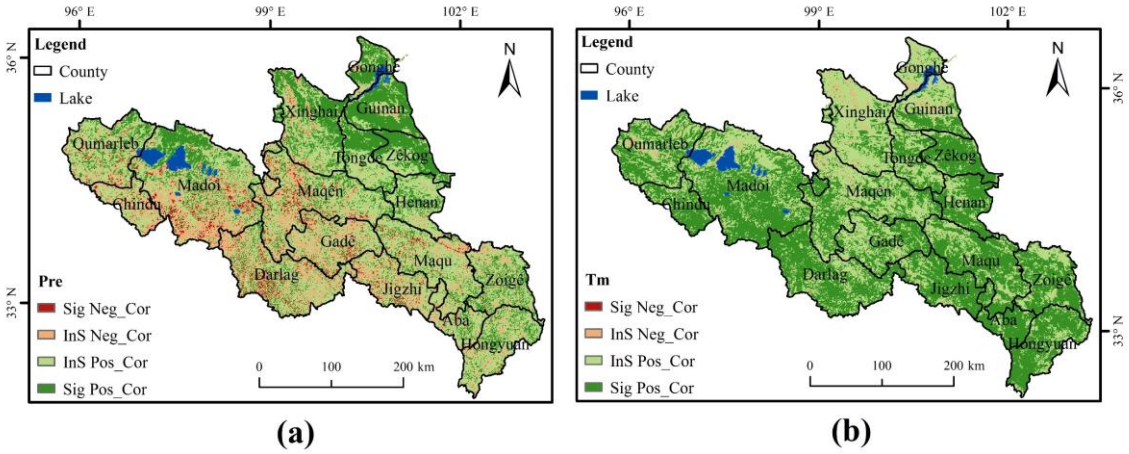

Figure 6. Spatial distribution of the correlation analysis for the NDVI and climate elements: (**a**) precipitation; (**b**) temperature. In the figure, Sig Neg_Cor represents a significant negative correlation; InS Neg_Cor represents a nonsignificant negative correlation; InS Pos_Cor represents a nonsignificant positive correlation; and Sig Pos_Cor represents a significant positive correlation.

3.3. Impact of Human Activities on NDVI

Numerous studies have shown that alpine vegetation, which is highly sensitive to global changes [39,40], has been severely affected by global climate change and human activities. The impact of human activities on vegetation changes mainly includes the promotion of increased vegetation cover (ecological engineering, etc.) and the destructive effect of reduced vegetation cover (grazing, urban expansion, etc.). Spatial distribution of the residual analysis for NDVI are shown in Figure 7. Eight typical areas were selected in the figure, and human activities information in these areas were collected to verify the residual results.

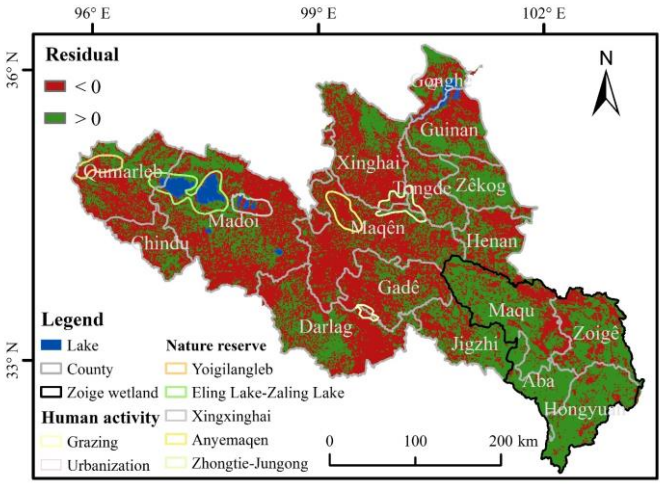

Figure 7. Spatial distribution of the residual analysis for NDVI.

Figure 7 shows that 53.58% of the residual values were negative, which mainly included the central and western regions in the SRYR, and Maqên accounted for the highest proportion. Human activities in these areas play a negative role in vegetation. The values in Maqên within the territory of the Anyemaqen Mountains, were sensitive and exhibited risk of change [41]. These areas are high-altitude regions with the following basic characteristics: poor water-heat conditions and strong solar radiation, which are not conducive to the implementation of ecological construction projects. The ecological environment continues to deteriorate. Second, at the border of Gadê and Darlag, human activity had a negative effect on vegetation. Over the last 19 years, the desertification and environmental

degradation of this region have mainly been attributed to human activities such as overgrazing, under the background of regional climate changes. Liu reported that grassland degradation was the most important land-cover change in the SRYR [42]. Furthermore, in the central part of Gonghe, land-use changes were caused by the rapid expansion of built-up land and had a negative effect on local vegetation.

In addition, 46.42% of the area exhibited positive residuals, mainly in the Zoigê wetland and nature reserves. Human activities in these areas play a positive role in vegetation. The Zoigê wetland mainly includes Hongyuan, Aba, Zoigê, and Maqu. The residuals in core areas of nature reserves [43] were positive, which mainly including Yoigilangleb, Eling Lake–Zaling Lake, and Zhongtie-Jungong. The NDVI values in these areas showed an increasing trend, indicating that decreasing trends of vegetation and expanding desertification were restrained, and wetland expansion and increasing vegetation cover were obvious. To a certain extent, the effects of the establishment of the Three-River-Source Nature Reserve (2000) were confirmed, and the ecological protection construction project (2005) has already achieved initial results. The establishment of the Three-River-Source National Park in 2020 indicated that the ecological protection of the Yellow River source area had reached a new level.

3.4. Trend Prediction

Multivariate linear regression equations were used to obtain the regression coefficients of the observed NDVI values and the observed climate elements (precipitation and temperature) from 1998 to 2016. The regression coefficients were fitted based on the climate forecast data from RegCM4 during the same period to simulate the pixel-based change trend of the NDVI. The comparison in Figure 8b shows that the simulated NDVI tendency value with linear tendencies of 0.00207/a, was the same as the observed NDVI tendency value with linear tendencies of 0.00204/a. This result shows that the credibility of the simulated NDVI trend was high. For the simulated future time period, we chose 2020–2038, which was similar to the past time length and close to the present time. Based on the grid, using the established pixel-scale NDVI-climate model, NDVI change trend distribution from 2020 to 2038 was analysed at the pixel scale with MATLAB. The statistics were calculated with the equation:

NDVI (2020–2038) = Precipitation regression coefficient (1998–2016) * precipitation (2020–2038) + Temperature regression coefficient (1998–2016) * temperature (2020–2038).

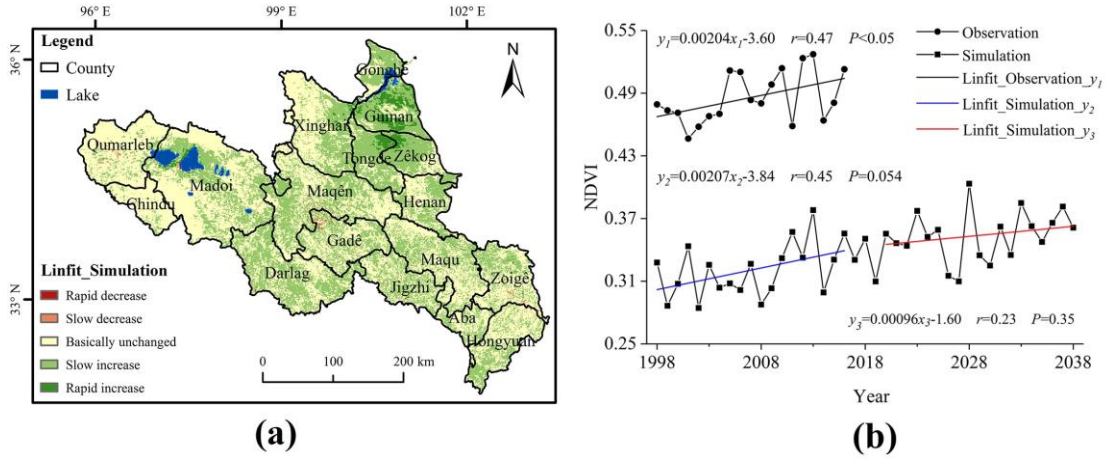

Figure 8. Prediction of the NDVI trend from 2020 to 2038: (**a**) spatial distribution; (**b**) temporal series. In the Figure 8a, rapid decrease represents a slope <–0.003; slow decrease represents –0.003 < slope < –0.001; basically unchanged represents –0.001 < slope < 0.001; slow increase represents 0.001 < slope < 0.003; rapid increase represents a slope <0.003.

According to Figure 8, the NDVI will show a slight upward trend over the next 19 years, with a slope of 0.00096/a. From 2020 to 2038, the areas where the NDVI will basically remain unchanged and slowly increase cover 54% and 42.43% of the total area, respectively. Among these areas, the basically unchanged areas are mainly distributed in Chindu and Qumarleb, the proportions of which are 91.16% and 86.15% in each county. The slowly increasing areas are mainly concentrated in Zêkog and Tongde, covering 70.76% and 69.83% of the county, respectively. In addition, NDVI has been increasing rapidly in the areas of Guinan, Zêkog and Tongde, where there is currently a large amount of cropland and a small amount of sandy land, following a similar trend over the past 19 years. The increasing NDVI trend in Guinan is the most obvious, with a rapid growth rate of 0.00267/a, covering 83.34% of the county.

The inputs to the prediction model are mainly precipitation and temperature, so the increase in NDVI is related to global warming. Rising temperatures, melting glaciers and increasing precipitation provide a good environment for vegetation cover. New studies have found that shrubs and grasses are springing up around Mount Everest [44], and the temperature in Antarctica exceeded 20 °C for the first time. These results suggest that Himalayan ecosystems are highly vulnerable to climate-induced shifts in vegetation, and the effects of global warming are spreading. Climate change affects vegetation growth, and vegetation change reflects climate variation. The SRYR is a sensitive area to climate, and the past and future trends of NDVI both demonstrate the warming and wetting trends of climate, which should arouse attention.

The climate simulation model was different from the weather forecast model and the short-term climate prediction model. The dates in the model were not equal to actual calendar dates. Therefore, the results of this study were only for the simulation of future NDVI trends and do not represent current NDVI values.

4. Discussion

The SRYR is an important water conservation and recharge area in the Yellow River basin due to its unique climatic characteristics and rich wetland system. We found that the NDVI increased over more than 70% of the study area, and the rate of increase ranged from 0 to 0.00559/a. Compared with that in 1998, the NDVI increased in the majority of the area in 2016. However, in considerable parts of Qumarleb and Maqên, the NDVI decreased, indicating that the natural ecological environment needs to be protected. He reported that grazing exclusion was an effective restoration approach to rehabilitate degraded alpine meadows in Maqin [45]. The annual precipitation in the study area increased from 1998 to 2016, with significant changes in different stages. The results were consistent with those of Li [46]. The temperature increased with a linear tendency of 0.0355/a. The annual average temperature increase over the past several years was mainly caused by the increase in the average annual minimum temperature [47]. Related studies have also confirmed that the climate in the SRYR is warming [26,47,48]. The temperature changes in the region over the past 19 years were consistent with those throughout China [49], and all regions showed increasing temperatures. However, the temperature increase was larger in the SRYR than the overall increases in China, which also confirmed the sensitivity of the alpine region to global changes [50]. This study showed that the temperature and precipitation of the SRYR have been increasing over the past 19 years. The climate of the region will enter a warmer and wetter period, which will be conducive to the restoration and establishment of vegetation. In addition, the NDVI was found to be more sensitive to temperature than precipitation.

In addition, the variations in grassland vegetation responded not only to long- and short-term changes in climate but also to the impact of human activities and their associated perturbations. State-approved ecological protection construction efforts involve major projects such as returning pastures to grasslands and ecological immigration. The implementation of continuous ecological restoration and ecological protection projects has increased the vegetation coverage to a certain extent, but the vegetation degradation caused by intensified human activities in local areas cannot be ignored.

The region has been overused and overgrazed for a long time throughout history. Overgrazing is the main factor causing the degradation of grassland ecosystems [41]. The residual results showed that human activities had a higher negative residual on the vegetation in the study area, indicating that the degradation of the alpine vegetation had not been effectively contained, which was consistent with the results of related research. The grassland NDVI was closely related to climate. Our research showed that the trend of the NDVI was most consistent with the grassland NDVI trend, and the partial correlation between the grassland NDVI and temperature was the best. Yang [49] selected the period from 1998–2007 to analyse the vegetation trends in the SRYR. The results showed that vegetation was improving [51], which is consistent with the results of this article. Ongoing climate change and human interference have greatly affected vegetation. Therefore, the wetting tendency of the climate and vegetation restoration projects might be the main reasons for vegetation improvements in the SRYR.

The prediction of the NDVI in the SRYR showed that it may increase over the next 19 years, which was consistent with the trends from 1998 to 2016. In addition to climate elements and human activities, NDVI is also affected by air pollution, soil degradation, slope and other factors. The quantification of the relationships between vegetation change and these factors has become difficult. The choice of data image resolution and time series and factors affecting NDVI will be the direction of our future research. Currently, the frequency of remote-sensing images has shifted from an annual scale to finer scales, such as monthly, ten-day, and daily periods. Methods for improving the spatial and temporal resolution quality of NDVI data through scientific data fusion methods by using high-resolution MODIS NDVI, high-resolution SPOT NDVI, and long time-series GIMMS NDVI data are worth exploring.

5. Conclusions

Based on the NDVI and climate data in the growing season from 1998 to 2016, this study analysed the spatial and temporal characteristics and impact mechanisms of the NDVI in the SRYR and predicted future NDVI trends. The results showed the following:

(1) The average NDVI in the growing season was 0.486, which decreased from northwest to southeast and showed obvious regional differences. The NDVI values were concentrated between 0.3 and 0.6 over 50.77% of the total area. The NDVI showed a trend of "increasing overall and decreasing locally", and 71.40% of the area showed an increasing trend. Among the different land-use types, woodland had the highest NDVI value, and the grassland NDVI trend coincided best with the overall NDVI trend.

(2) From 1998 to 2016, both precipitation and temperature showed an increasing trend. These conditions may be the main reason for the warm and humid climate in the SRYR in recent years. This trend was conducive to the improvement of vegetation. The sensitivity of vegetation and temperature was higher than that of precipitation. Among the different counties, the effects on vegetation were more obvious under unfavourable climate conditions than under suitable ones. The results of the residual analysis indicated that human activities had a positive impact on 46.42% of the SRYR. However, 53.58% of the area was still negatively affected by human activities, which proves that the trend of grassland degradation had not been effectively contained.

(3) The trend simulation results suggested that the NDVI showed a slight upward trend from 2020 to 2038. The NDVI has been increasing rapidly in the areas of Guinan, Zêkog and Tongde. The past and future NDVI trends in the SRYR both demonstrate climate warming and wetting trends, which should arouse attention.

Due to the limitations in data coverage for earlier years, this article analysed the spatiotemporal changes in the source area over only the last 19 years and simulated the trends for the next 19 years. Studies on long time-series data are the next research direction.

Author Contributions: Mingyue Wang and Jun'e Fu conceived the general idea and designed the experiments. Mingyue Wang and Zhitao Wu performed the experimens. Mingyue Wang, Jun'e Fu and Zhiguo Pang made the dataset. Mingyue Wang wrote the whole paper, and all authors participated in the analysis of results and edited the paper. All authors have read and agreed to the published version of the manuscript.

Funding: This work was supported by the National Key Point Research and Invention Program of the Thirteenth Five Year Plan (2017YFA0605003), and the Natural Science Foundation of China (51779269).

Acknowledgments: The authors would like to thank work fellows of Research Center on Flood & Drought Disaster Reduction of the Ministry of Water Resources for their support during this research. Meanwhile, thanks to the five anonymous reviewers and all the editors who contributed with their comments and suggestions to improve the quality of the manuscript in the process of revision.

Conflicts of Interest: The authors declare no conflicts of interest.

References

1. Hughes, T.P.; Kerry, J.T.; Connolly, S.R.; Baird, A.H.; Eakin, C.M.; Heron, S.F.; Hoey, A.S.; Hoogenboom, M.O.; Jacobson, M.; Liu, G.; et al. Ecological memory modifies the cumulative impact of recurrent climate extremes. *Nat. Clim. Chang.* **2019**, *9*, 40–43. [CrossRef]
2. Walther, G.R.; Post, E.; Convey, P.; Menzel, A.; Parmesan, C.; Beebee, J.C.; Fromentin, J.M.; Ove, H.G.; Bairlein, F. Ecological responses to recent climate change. *Nature* **2002**, *416*, 389–395. [CrossRef] [PubMed]
3. Wang, C.; Sun, Y.; Li, L.; Zhang, Q. Quantitative evaluation of regional vegetation ecological environment quality by using remotely sensed data over Qingjiang, Hubei. In Proceedings of the SPIE Second International Conference on Space Information Technology, Wuhan, China, 10 November 2007; Volume 6795.
4. Zhong, B.X.; Jiong, X.X.; Wei, Z. Spatiotemporal variations of vegetation cover on the Chinese Loess Plateau (1981–2006): Impacts of climate changes and human activities. *Sci. China Ser. D Earth Sci.* **2008**, *51*, 67–78.
5. Qin, Z.H.; Zhu, Y.X.; Li, W.J.; Xu, B. Mapping vegetation cover of grassland ecosystem for desertification monitoring in Hulun Buir of Inner Mongolia, China. In Proceedings of the Remote Sensing for Agriculture, Ecosystems, and Hydrology, Cardiff, Wales, UK, 16–18 September 2008; Volume 7104.
6. Xu, C.; Li, Y.T.; Hu, J.; Yang, X.J.; Sheng, S.; Liu, M.S. Evaluating the difference between the normalized difference vegetation index and net primary productivity as the indicators of vegetation vigor assessment at landscape scale. *Environ. Monit. Assess.* **2011**, *184*, 1275–1286. [CrossRef] [PubMed]
7. Kawabata, A.; Ichii, K.; Yamaguchi, Y. Global monitoring of interannual changes in vegetation activities using NDVI and its relationships to temperature and precipitation. *Int. J. Remote Sens.* **2001**, *22*, 1377–1382. [CrossRef]
8. Liu, X.F.; Zhu, X.F.; Pan, Y.Z.; Li, Y.Z.; Zhao, A.Z. Spatiotemporal changes in vegetation coverage in China during 1982–2012. *Acta Ecol. Sin.* **2015**, *35*, 5331–5342. (In Chinese)
9. Piao, S.L.; Fang, J.Y. Dynamic vegetation cover change over the last 18 years in China. *Quat. Sci.* **2001**, *4*, 294–302. (In Chinese)
10. Xu, G.C.; Zhang, J.X.; Li, P.; Li, Z.B.; Lu, K.X.; Wang, X.K.; Wang, F.C.; Cheng, Y.T.; Wang, B. Vegetation restoration projects and their influence on runoff and sediment in China. *Ecol. Indic.* **2018**, *95*, 233–241. [CrossRef]
11. Zhang, D.D.; Yan, D.H.; Wang, Y.C.; Lu, F.; Wu, D. Changes in extreme precipitation in the Huang-Huai-Hai River basin of China during 1960–2010. *Theor. Appl. Climatol.* **2015**, *120*, 195–209. [CrossRef]
12. Cui, L.F.; Wang, L.C.; Singh, R.P.; Lai, Z.P.; Jiang, L.L.; Yao, R. Association analysis between spatiotemporal variation of vegetation greenness and precipitation/temperature in the Yangtze River Basin (China). *Environ. Sci. Pollut. Res.* **2018**, *25*, 21867–21878. [CrossRef]
13. Xu, W.X.; Liu, X.D. Response of Vegetation in the Qinghai-Tibet Plateau to Global Warming. *Chin. Geogr. Sci.* **2007**, *17*, 151–159. [CrossRef]
14. Hou, W.J.; Gao, J.B.; Wu, S.H.; Dai, E.F. Interannual Variations in Growing-Season NDVI and Its Correlation with Climate Variables in the Southwestern Karst Region of China. *Remote Sens.* **2015**, *7*, 11105–11124. [CrossRef]
15. Jin, H.; He, R.; Cheng, G.; Wu, Q.; Wang, S.; Lü, L.; Chang, X. Changes in frozen ground in the Source Area of the Yellow River on the Qinghai–Tibet Plateau, China, and their eco-environmental impacts. *Environ. Res. Lett.* **2009**, *4*, 45206. [CrossRef]

16. Li, J.; Sheng, Y.; Wu, J.C.; Feng, Z.L.; Ning, Z.J.; Hu, X.Y.; Zhang, X.M. Landform-related permafrost characteristics in the source area of the Yellow River, eastern Qinghai-Tibet Plateau. *Geomorphology* **2016**, *269*, 104–111. [CrossRef]
17. Hu, G.Y.; Jin, H.J.; Dong, Z.B.; Lu, J.F.; Yan, C.Z. Driving forces of aeolian desertification in the source region of the Yellow River: 1975–2005. *Environ. Earth Sci.* **2013**, *70*, 3245–3254. [CrossRef]
18. Zhang, H.W. Ecological protectionand high-quality development in the yellow river basin are guaranteed by scientific management methods. *Yellow River* **2020**, *42*, 148–155. (In Chinese)
19. Qin, Y.; Yang, D.; Gao, B.; Wang, T.; Chen, J.; Chen, Y.; Zheng, G. Impacts of climate warming on the frozen ground and eco-hydrology in the Yellow River source region, China. *Sci. Total Environ.* **2017**, *605*, 830–841. [CrossRef]
20. Mudassar, I.; Wen, J.; Wang, S.P.; Tian, H.; Muhammad, A. Variations of precipitation characteristics during the period 1960–2014 in the Source Region of the Yellow River, China. *J. Arid Land* **2018**, *10*, 388–401.
21. Yang, J.P. Studies on eco-environmental change in source regions of the Yangtze and Yellow Rivers of China: Present and future. *Sci. Cold Arid Reg.* **2019**, *11*, 173–183.
22. Jiang, C.; Zhang, L.B. Climate Change and Its Impact on the Eco-Environment of the Three-Rivers Headwater Region on the Tibetan Plateau, China. *Int. J. Environ. Res. Public Health* **2015**, *12*, 12057–12081. [CrossRef]
23. Guo, W.Q.; Yang, T.B.; Dai, J.G.; Shi, L.; Lu, Z.Y. Vegetation cover changes and their relationship to climate variation in the source region of the Yellow River, China, 1990–2000. *Int. J. Remote Sens.* **2008**, *29*, 2085–2103. [CrossRef]
24. Liang, S.H.; Ge, S.M.; Wan, L.; Xu, D.W. Characteristics and causes of vegetation variation in the source regions of the Yellow River, China. *Int. J. Remote Sens.* **2012**, *33*, 1529–1542. [CrossRef]
25. Adnani, A.E.; Habib, A.; Khalidi, K.E.; Zourarah, B. Spatio-Temporal Dynamics and Evolution of Land Use Land Cover Using Remote Sensing and GIS in Sebou Estuary, Morocco. *J. Geogr. Inf. Syst.* **2019**, *11*, 551–566. [CrossRef]
26. Iqbal, M.; Wen, J.; Lan, Y.C.; Anjum, M.N.; Adnan, M.; Wang, X.; Tian, H. Assessment of Air Temperature Trends in the Source Region of Yellow River and Its Sub-Basins, China. *Asia-Pac. J. Atmos. Sci.* **2018**, *54*, 111–123. [CrossRef]
27. Hu, Y.R.; Maskey, S.; Uhlenbrook, S.; Zhao, H.L. Streamflow trends and climate linkages in the source region of the Yellow River, China. *Hydrol. Process.* **2011**, *25*, 3399–3411. [CrossRef]
28. Li, L.; Shen, H.Y.; Dai, S.; Xiao, J.S.; Shi, X.H. Response of runoff to climate change and its future tendency in the source region of Yellow River. *J. Geogr. Sci.* **2012**, *22*, 431–440. [CrossRef]
29. Xu, X.L. China Monthly Vegetation Index (NDVI) spatial distribution data set. In *Data Registration and Publishing System of the Resource and Environmental Data Cloud Platform Centre of the Chinese Academy of Sciences*; Resource and Environmental Data Cloud Platform Centre of the Chinese Academy of Sciences: Beijing, China, 2020. (In Chinese)
30. Xu, Y.; Gao, X.J.; Shen, Y.; Xu, C.H.; Shi, Y.; Giorgi, F. A Daily Temperature Dataset over China and Its Application in Validating a RCM Simulation. *Adv. Atmos. Sci.* **2009**, *26*, 763–772. [CrossRef]
31. Wu, J.; Gao, X.J. Simulation of tropical cyclones over the western north pacific and landfalling in China by REGCM4. *J. Trop. Meteorol.* **2019**, *25*, 437–447.
32. Chu, L.; Huang, C.; Liu, G.H.; Liu, Q.S.; Zhao, J. Analysis on vegetation changes of Maqu alpine wetlands in the Yellow River source region. In Proceedings of the Land Surface Remote Sensing II, Beijing, China, 13–16 October 2014; Volume 9260.
33. Pirnia, A.; Darabi, H.; Choubin, B.; Omidvar, E.; Onyutha, C.; Haghighi, A.T. Contribution of climatic variability and human activities to stream flow changes in the Haraz River basin, northern Iran. *J. Hydro-Environ. Res.* **2019**, *25*, 12–24. [CrossRef]
34. Evans, J.; Geerken, R. Discrimination between climate and human-induced dryland degradation. *J. Arid Environ.* **2004**, *57*, 535–554. [CrossRef]
35. Chen, H.; Liu, X.N.; Ding, C.; Huang, F. Phenology-Based Residual Trend Analysis of MODIS-NDVI Time Series for Assessing Human-Induced Land Degradation. *Sensors* **2018**, *18*, 3676. [CrossRef] [PubMed]
36. Yuan, L.H.; Chen, X.Q.; Wang, X.Y.; Xiong, Z.; Song, C.Q. Spatial associations between NDVI and environmental factors in the Heihe River Basin. *J. Geogr. Sci.* **2019**, *29*, 1548–1564. [CrossRef]
37. Morecroft, M.D.; Paterson, J.S. Effects of temperature and precipitation changes on plant communities. *Plant Growth Clim. Chang.* **2006**, *16*, 146–164.

38. Nemani, R.; Keeling, C.; Hashimoto, H.; Jolly, W.; Piper, S.; Tucker, C.; Myneni, R.; Running, S. Climate-driven increases in global terrestrial net primary production from1982 to 1999. *Science* **2003**, *300*, 1560–1563. [CrossRef]
39. Liu, S.L.; Zhao, H.D.; Su, X.K.; Deng, L.; Dong, S.K.; Zhang, X. Spatio-temporal variability in rangeland conditions associated with climate change in the Altun Mountain National Nature Reserve on the Qinghai-Tibet Plateau over the past 15 years. *Rangel. J.* **2015**, *37*, 67. [CrossRef]
40. McGuire, A.D.; Sturm, M.; Chapin, F.S., III. Arctic Transitions in the Land–Atmosphere System (ATLAS): Background, objectives, results, and future directions. *J. Geophys. Res.-Atmos.* **2003**, *108*. [CrossRef]
41. Peng, J.F.; Gou, X.H.; Chen, F.H.; Li, J.B.; Liu, P.B.; Zhang, Y. Altitudinal variability of climate–tree growth relationships along a consistent slope of Anyemaqen Mountains, northeastern Tibetan Plateau. *Dendrochronologia* **2008**, *26*, 87–96. [CrossRef]
42. Liu, L.S.; Zhang, Y.L.; Bai, W.Q.; Yan, J.Z.; Ding, M.J.; Shen, Z.X.; Li, S.C.; Zheng, D. Characteristics of grassland degradation and driving forces in the source region of the Yellow River from 1985 to 2000. *J. Geogr. Sci.* **2006**, *16*, 131–142. [CrossRef]
43. Shao, Q.Q.; Liu, J.Y.; Huang, L.; Fan, J.W.; Xu, X.L.; Wang, J.B. Integrated assessment on the effectiveness of ecological conservation in Sanjiangyuan National Nature Reserve. *Geogr. Res.* **2013**, *32*, 1645–1656. (In Chinese)
44. Anderson, K.; Fawcett, D.; Cugulliere, A.; Benford, S.; Jones, D.; Leng, R. Vegetation expansion in the subnival Hindu Kush Himalaya. *Glob. Chang. Biol.* **2020**, *26*, 1608–1625. [CrossRef]
45. He, H.; Li, H.; Zhu, J.; Mao, S.; Li, Y.; Yang, Y.; Zhang, F. Effects of Grazing Exclusion on Soil Properties in Maqin Alpine Meadow, Tibetan Plateau, China. *Pol. J. Environ. Stud.* **2016**, *25*, 1583–1587.
46. Li, Q.; Yang, M.X.; Wan, G.N.; Wang, X.J. Spatial and temporal precipitation variability in the source region of the Yellow River. *Environ. Earth Sci.* **2016**, *75*, 594. [CrossRef]
47. Hu, Y.; Maskey, S.; Uhlenbrook, S. Trends in temperature and rainfall extremes in the Yellow River source region, China. *Clim. Chang.* **2012**, *110*, 403–429. [CrossRef]
48. Chen, L.; Chang, J.X.; Wang, Y.M. Assessing runoff sensitivities to precipitation and temperature changes under global climate-change scenarios. *Hydrol. Res.* **2018**, *50*, 24–42. [CrossRef]
49. Du, Q.Q.; Zhang, M.J.; Wang, S.J. Changes in air temperature over China in response to the recent global warming hiatus. *Acta Geogr. Sin.* **2019**, *29*, 496–516. [CrossRef]
50. Chen, F.; Zhang, Y.; Shao, X.M.; Li, M.Q.; Yin, Z.Y. A 2000-year temperature reconstruction in the Animaqin Mountains of the Tibet Plateau, China. *Holocene* **2016**, *26*, 1904–1913. [CrossRef]
51. Yang, Z.P.; Gao, J.X.; Zhou, C.P.; Shi, P.L.; Zhao, L.; Shen, W.S.; Ouyang, H. Spatio-temporal changes of NDVI and its relation with climatic variables in the source regions of the Yangtze and Yellow rivers. *J. Geogr. Sci.* **2011**, *21*, 979–993. [CrossRef]